JACS
JOURNAL OF THE AMERICAN CHEMICAL SOCIETY

Article

pubs.acs.org/JACS

Metal–Organic Polyhedral Core as a Versatile Scaffold for Divergent and Convergent Star Polymer Synthesis

Nobuhiko Hosono,*[,†] Mika Gochomori,[†] Ryotaro Matsuda,[†,#] Hiroshi Sato,[†,§] and Susumu Kitagawa*[,†,‡]

[†]Institute for Integrated Cell-Material Sciences (WPI-iCeMS), Kyoto University, Katsura, Nishikyo-ku, Kyoto 615-8530, Japan

[‡]Department of Synthetic Chemistry and Biological Chemistry, Graduate School of Engineering, Kyoto University, Katsura, Nishikyo-ku, Kyoto 615-8510, Japan

Supporting Information

ABSTRACT: We herein report the divergent and convergent synthesis of coordination star polymers (CSP) by using metal–organic polyhedrons (MOPs) as a multifunctional core. For the divergent route, copper-based great rhombicuboctahedral MOPs decorated with dithiobenzoate or trithioester chain transfer groups at the periphery were designed. Subsequent reversible addition–fragmentation chain transfer (RAFT) polymerization of monomers mediated by the MOPs gave star polymers, in which 24 polymeric arms were grafted from the MOP core. On the other hand, the convergent route provided identical CSP architectures by simple mixing of a macroligand and copper ions. Isophthalic acid-terminated polymers (so-called macroligands) immediately formed the corresponding CSPs through a coordination reaction with copper(II) ions. This convergent route enabled us to obtain miktoarm CSPs with tunable chain compositions through ligand mixing alone. This powerful method allows instant access to a wide variety of multicomponent star polymers that conventionally have required highly skilled and multistep syntheses. MOP-core CSPs are a new class of star polymer that can offer a design strategy for highly processable porous soft materials by using coordination nanocages as a building component.

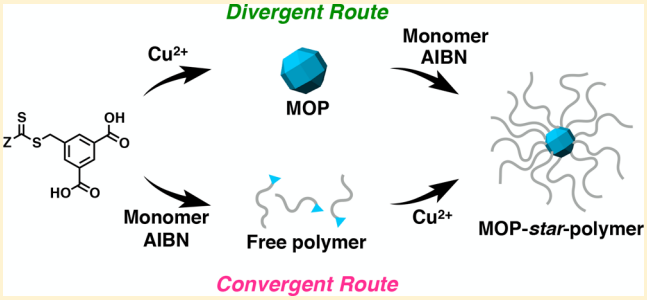

INTRODUCTION

Tailoring macromolecular architecture is a grand challenge for polymer chemistry.[1] Following the discovery of living polymerization in the middle of the last century,[2] advances in polymer chemistry have provided us with a variety of synthetic polymers with complex architectures, including block copolymers, gradient copolymers, cyclic polymers, graft (comb) polymers, dendrimers, and star polymers.[1] In particular, star polymers,[3−6] which are a class of multiarmed macromolecules with more than three "arm chains" connected at an identical center, have attracted significant interest due to not only their topological importance but also their unique physical properties originating from their compact macromolecular shape. For instance, because of the radiating architecture, intermolecular entanglements are suppressed, resulting in an extremely low viscosity compared with their linear analogues with similar molecular weights.

Conventional star polymers are synthesized via either divergent or convergent approaches. The divergent approach entails conventional living polymerization with multifunctional initiators.[3] On the other hand, the convergent approach involves covalent,[4] supramolecular,[5] and coordination bond[6] formation to couple end-functionalized polymeric precursors with multifunctional cores. Whereas the divergent route is advantageous for synthetic precision, the convergent route is more accessible because of its facile synthetic protocol, as well as the structural versatility of the resulting macromolecular architectures. A combination of both approaches is generally employed for the synthesis of miktoarm star polymers.[7] Miktoarm star polymers, in which two or more chemically different arms radiate from an identical core, are an important subclass of star polymers.[7b] Due to their segmented block architectures, miktoarm stars have been extensively studied with regard to self-assembly in the bulk and in solution. However, the syntheses of these systems have required multiple protecting/deprotecting steps, orthogonal coupling reactions, and different polymerization methods.[7b]

Recently, porous coordination polymers (PCPs) and metal–organic frameworks (MOFs) have received considerable attention as new classes of porous materials that are constructed through self-assembly of organic ligands and metal ions.[8] Metal–organic polyhedrons (MOPs) or coordination nanocages are discrete cage-like analogues of PCPs and MOFs.[9] MOPs have been used as building blocks for MOF frameworks[10] or molecular containers,[11] and as fillers of mixed-matrix membranes for gas separation applications.[12] In the present work, we disclose a new class of star polymers, termed coordination star polymers (CSPs), which has a MOP core at the center. Coordination-driven self-assembly, which has been utilized extensively for the synthesis of dendrimers and

Received: February 17, 2016
Published: April 27, 2016

DOI: 10.1021/jacs.6b01758
J. Am. Chem. Soc. 2016, 138, 6525−6531

molecular capsules,[13] plays a crucial role in structuring the star polymer architecture. This approach facilitates the synthesis of star polymers, including multicomponent miktoarm stars, which has often been constrained by the need for time-consuming procedures and highly skilled polymerization techniques.

The MOP-core CSPs were synthesized via both divergent (core-first) and convergent (arm-first) routes. For the divergent route, we employed great rhombicuboctahedral MOPs as a multifunctional core that consists of a total of 24 isophthalic acid ligands interconnected via 12 dicopper paddlewheel clusters (Figure 1). The organic ligands were substituted with

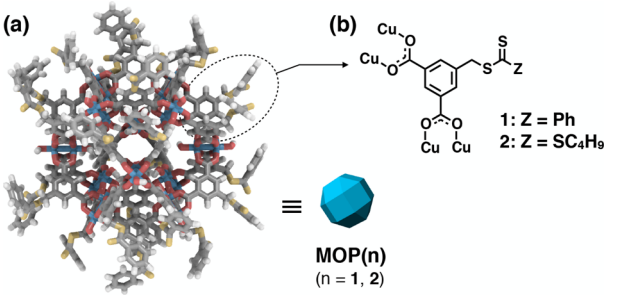

Figure 1. (a) Modeled structure of **MOP(1)**; **Z** = Ph. (b) Chemical structure of the building subunit of **MOP(*n*)** (*n* = **1** and **2**), which carries a chain transfer group.

dithiobenzoate or trithioester chain transfer groups in order to graft polymer chains to the periphery of the MOP. Reversible addition–fragmentation chain transfer (RAFT) polymerization[14] mediated with the MOP led to MOP-core star polymers, in which a total of 24 arm chains were grafted to a single core.

Meanwhile, we discovered that a convergent approach was also feasible for this system. Presynthesized linear polymers with isophthalic acid end groups (so-called macroligands) instantly gave the corresponding MOP-core CSP through a coordination reaction with copper(II) ions. By using a mixture of ligands, this convergent route provided a variety of miktoarm star polymers with the desired arm compositions via one-step solution mixing. Furthermore, the number of arm chains in the star polymer could be easily tuned in the range of 5–24 by simply adjusting the mixing ratio between the macroligand and low-molecular weight coligand.

In contrast to conventional covalent star polymers, the MOP-core CSPs were easily dissociated into their free arm chains by the addition of acid or a competing copper-chelating agent, which enabled us to fully characterize the absolute molecular weight and number of arm chains in the star polymers. The powerful approach developed in this study offers access to a wide variety of star polymers, including miktoarm stars with the desired number and composition of arm chains, without complex synthesis. Moreover, as clearly demonstrated by the established use of PCPs and MOFs,[8] the cavity in the MOP core has obvious potential as a functional space for reactions, catalysis, drug containment,[11] and gas separation applications.[12] Selection of the arm polymers, as well as the precise control of the arm length, can be used to tune the physical properties, such as thermophysical properties, of the MOP-core CSPs on demand. This would lead to highly processable porous soft materials using MOPs as the building components, whereas the formation of malleable materials from analogous PCPs or MOFs is generally difficult because of their crystalline nature.

RESULTS AND DISCUSSION

Divergent Route. For the divergent approach, we employed a RAFT[14] polymerization method because it requires no metal catalyst, which could disturb the coordination framework of the MOP core. We designed isophthalic acid ligands substituted with dithiobenzoate (**1**, **Z** = Ph) and trithioester (**2**, **Z** = SCH_4H_9), which are typical chain transfer (CT) moieties for RAFT (Figure 1). The coordination reaction between **1** and copper(II) acetate in *N*-methylpyrrolidone (NMP) instantly provided a MOP, **MOP(1)**. The formation of **MOP(1)** was monitored *in situ* by size-exclusion chromatography (SEC) using THF as the eluent (Figure S1). After mixing **1** with an equimolar amount of copper(II) acetate in NMP, the peak of **1** in SEC disappeared within 5 min and a new higher-molecular-weight peak of 4070 g/mol (relative to polystyrene standards) with exceptionally narrow polydispersity ($Đ = M_w/M_n = 1.02$) appeared (Figure S1). This observation is a strong indication of the formation of **MOP(1)**. The product was readily isolated by precipitation from methanol. **MOP(2)** ($M_{n,MOP}$ (SEC) = 5090, $Đ = 1.02$) was prepared in the same way using **2**, although additional purification by preparative SEC was needed. During the reaction of **2** and copper(II) acetate, a small amount of unidentified byproduct with a higher molecular weight was formed (Figure S2). This is presumably due to a trace amount of a difunctional impurity of **2**, *S*,*S*′-di(5-methylisophthalic) trithiocarbonate, as detected by ESI-MS (Figure S3).

For comparison, a known MOP, **MOP(*t*Bipa)**,[9e] was measured by SEC. This MOP is composed of 5-*tert*-butylisophthalic acid (***t*Bipa**) with copper(II) ions, and its structure has been determined by single-crystal X-ray diffraction.[9e] As expected, SEC of **MOP(*t*Bipa)** gave a monodisperse peak at $M_{n,MOP}$ (SEC) = 3490 ($Đ = 1.01$) (Figure S1). It should be noted that SEC always gives a lower molecular weight (M) value than that expected for MOPs because of their compact spherical shape. In fact, the actual M values, $M_{n,MOP}$ (calcd), for **MOP(1)**, **MOP(2)**, and **MOP(*t*Bipa)** are 9454, 9744, and 6810 g/mol, respectively, based on the molecular formula. Both **MOP(1)** and **MOP(2)** were slightly soluble in THF, which allowed us to characterize them by electronic absorption spectroscopy. The isolated MOPs showed an absorption band at ~690 nm attributed to band(I) of the dinuclear copper(II) paddlewheel cluster (Figure S4), which is characteristic of typical copper-based MOPs.[9c] Elemental analysis suggested reasonable formulas for the MOPs that included coordinated solvents, as indicated by specific weight losses in the thermogravimetric (TG) analysis (Figure S5). However, all crystallization attempts gave amorphous products, which could be due to the bulky and flexible CT moieties dangling at the periphery of the MOPs.

Surface-initiated RAFT polymerization of *tert*-butyl acrylate (*t*BA) mediated with **MOP(2)** was performed in THF in the presence of 2,2′-azobis(isobutyronitrile) (AIBN) (Figure 2a). The SEC traces and kinetic plots of the polymerization are shown in Figure 2b,d, respectively. After an induction period of ~20 min, the **MOP(2)** peak in SEC shifted to the higher-molecular-weight region with reaction time, which indicates the successfully elongation of the polymeric arms from the **MOP(2)** surface under RAFT equilibrium. The reaction was stopped at 135 min to obtain poly(*t*BA)-grafted **MOP(2)** (termed **MOP(2)-P*t*BA39** CSP, $M_{n,MOP}$ (SEC) = 59200, $Đ = 1.04$) bearing P*t*BA arm chains with a degree of polymerization (DP) of 39 (Table 1). As evidenced by the kinetic plots (Figure 2d),

DOI: 10.1021/jacs.6b01758
J. Am. Chem. Soc. 2016, 138, 6525–6531

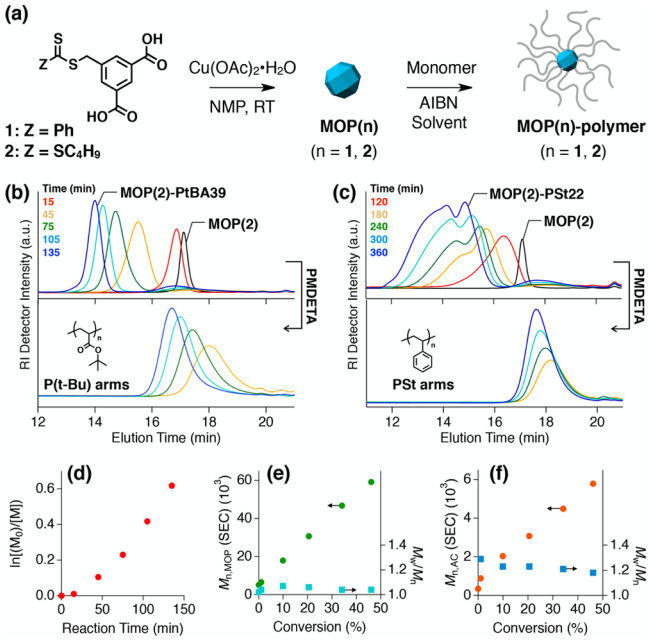

Figure 2. (a) Schematic diagram of the divergent route for MOP-core CSPs. The number of arm chains was reduced by half in the illustration for clarity. (b,c) SEC traces of RAFT polymerization mediated with **MOP(2)** (THF, 60 °C) for (b) *t*BA and (c) St. SEC traces of (top) graft polymerizations at given reaction times and (bottom) free arm chains prepared by addition of PMDETA to the reaction mixture. (d–f) Results of the RAFT polymerization of *t*BA meditated with **MOP(2)**: (d) kinetic plots; dependence of (e) $M_{n,MOP}$ (SEC) and (f) $M_{n,AC}$ (SEC) on the monomer conversion with respective M_w/M_n.

the polymerization was well controlled. The SEC peaks of **MOP(2)-P*t*BA** were quite narrow ($Đ$ < 1.1) and unimodal for conversions up to 50% (Figure 2b,e), although the molecular weights and dispersities determined by polystyrene-calibrated SEC do not reliably indicate the actual values for MOP-core CSPs. The number density of arm chains on the MOP-core CSP is expected to be 24 per core. It should be noted that a small amount of free polymer inevitably coexists with the MOP-core CSPs because of the RAFT equilibrium.[4c]

By tuning the monomer feed and reaction time, we could easily control the arm length and obtain **MOP(2)−P*t*BA15** with a much smaller size ($M_{n,MOP}$ (SEC) = 23600, $Đ$ = 1.06). The hydrodynamic diameters of **MOP(2)**, **MOP(2)−P*t*BA15**, and **MOP(2)−P*t*BA39** were determined by dynamic light scattering (DLS) in THF to be 7.3, 9.9, and 16.8 nm, respectively (Figure S6).

The MOP core can be broken apart into its free arm chains by the addition of a competitive copper chelator, *N*,*N*,*N*′,*N*″,*N*″-pentamethyldiethylenetriamine (PMDETA), which enabled us to characterize the arm chains *in situ* using SEC and NMR (see Supporting Information). After the addition of PMDETA (ca. 20 μL of 0.1 M THF solution to ca. 5 mg/mL CSP solution), **MOP(2)−P*t*BA39** disappeared immediately, as observed by SEC, to leave the free arm chains, **P*t*BA39** ($M_{n,AC}$ (SEC) = 5780, $Đ$ = 1.18, Figure 1b). The dependence of $M_{n,AC}$ (SEC), thus measured by *in situ* decomposition of **MOP(2)−P*t*BA**, on the conversion (Figure 2f) indicated successful control over the elongation reaction of the arm chains.

Interestingly, the polydispersity of the free arm chains is somewhat wider ($Đ$ > 1.1) than that of the original CSP, which probably originates from the compact star architecture and statistical convolution of the polydispersities (*vide infra*). SEC and ^{1}H NMR measurements after the decomposition showed no unreacted ligand, **2**, indicating that all 24 ligands of the MOP core were converted into polymeric arms. The absorption band observed at 690 nm for **MOP(2)−P*t*BA39** does not change significantly compared with that of **MOP(2)** (Figure S4), indicating that the MOP core is intact after the polymerization. The total molecular weight of **MOP(2)−P*t*BA39** was calculated to be $M_{n,MOP}$ (calcd) = 130400, whereas $M_{n,MOP}$ (SEC) was 59200. Using SEC-multiangle light scattering (MALS) analysis, the absolute weight-averaged M, $M_{w,MOP}$ (SEC-MALS), of **MOP(2)−P*t*BA39** was determined to be 157400, which is quite consistent with the calculated value.

In the present acrylate system, radical combination termination does not seem to be a major side reaction because no significant star−star coupling product was observed by SEC (Figure 2b). However, it should be noted that other side reactions, such as intramolecular radical transfer resulting in midchain radical (MCR) formation, might be operative.[15] These reactions may affect the inherent microstructures of CSPs by forming extra side-branches as well as star−star coupling *in situ*. In fact, the small high-molecular-weight shoulder observed for **MOP(2)−P*t*BA39** could be indicative of such larger byproducts (Figure 2b) (*vide infra*).

In contrast to *t*BA, the RAFT polymerization of styrene (St) mediated with **MOP(2)** appeared unsuccessful. The SEC traces

Table 1. Results for the Synthesis of MOP-Core CSPs through Divergent (Core-First) and Convergent (Arm-First) Approaches

	MOP				Arm Chain			
sample	$M_{n,MOP}$ (SEC)[a]	$Đ$[b]	$M_{n,MOP}$ (calcd)[c]	approach[d]	$M_{n,AC}$ (SEC)[a]	$Đ$[b]	$M_{n,AC}$ (NMR)[e]	DP (NMR)[f]
MOP(2)−P*t*BA15	23600	1.06	56200	→	2340	1.24	2280	15.1
MOP(2)−P*t*BA39	59200	1.04	130400	→	5780	1.18	5370	39.2
MOP(2)−PSt22	45300[g]	1.67[g]	65500	→	2570	1.23	2670	22.3
MOP(P*t*BA54)	62900	1.03	175000	←	6700	1.11	7230	53.7
MOP(P*t*BA148)	138700	1.04	521200	←	12700	1.25	19250	147.5
MOP(P*t*BA272)	226300	1.10	845000	←	21800	1.27	35140	271.5
MOP(P*n*BA14)	21500	1.04	51900	←	1880	1.22	2100	13.7
MOP(P*n*BA56)	62600	1.03	182100	←	6100	1.23	7520	56.0
MOP(P*n*BA56$_{0.6}$/P*t*BA272$_{0.4}$)	162100	1.07	434000	←	incorporation ratio, **P*n*BA56/P*t*BA272** = 0.62/0.38			

[a]Determined by SEC using THF as the eluent, calibrated with polystyrene standards. [b]M_w/M_n. [c]Molecular weight of MOP-core CSP calculated as $M_{n,MOP}$ (calcd) = ($M_{n,AC}$ (NMR) + 63.5) × 24. [d]Synthetic approach: divergent (→); convergent (←). [e]Molecular weight of free polymers calculated as $M_{n,AC}$ (NMR) = DP × molecular weight of monomer + molecular weight of CT ligand. [f]Degree of polymerization (DP) determined by NMR. [g]Multimodal distribution.

DOI: 10.1021/jacs.6b01758
J. Am. Chem. Soc. 2016, 138, 6525−6531

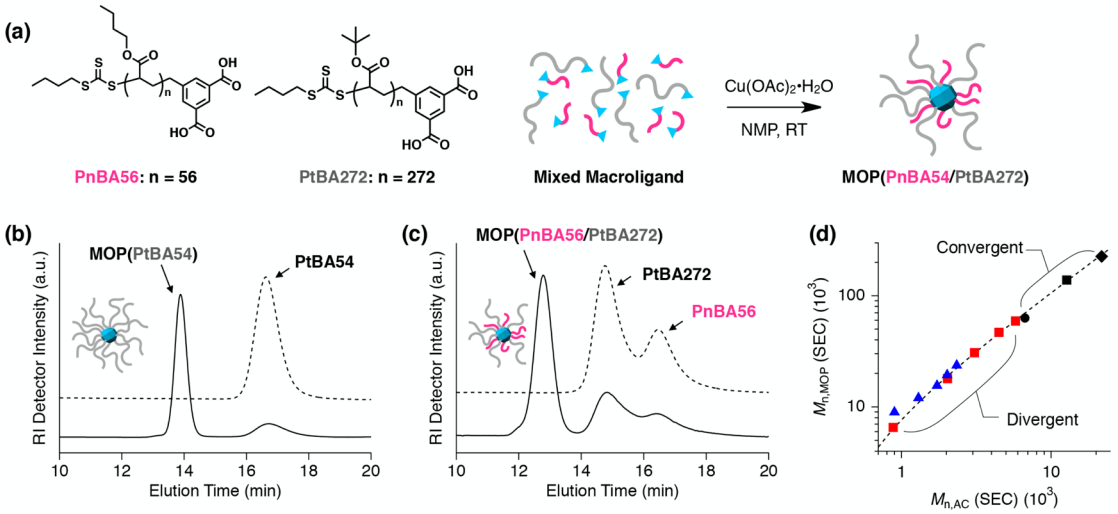

Figure 3. (a) Schematic diagram of the convergent route to the **P*n*BA56**/**P*t*BA272** binary miktoarm star polymer. The number of arm chains was reduced by half in the illustrations for clarity. (b) SEC traces of **P*t*BA54** (dashed line) and the reaction mixture of **P*t*BA54** and copper(II) acetate (1.5 equiv) in NMP after 60 min (solid line). (c) SEC traces of a binary solution of **P*n*BA56** and **P*t*BA272** with a mixing ratio of 0.6:0.4 (dashed line) and the reaction mixture of **MOP(P*n*BA56$_{0.6}$/P*t*BA272$_{0.4}$)** and copper(II) acetate (1.5 equiv) in NMP after 60 min (solid line). (d) Double logarithm plot of the relationship between $M_{n,MOP}$ and $M_{n,AC}$ determined by THF-SEC. The results of the divergent synthesis of **MOP(2)**−**P*t*BA15** and **MOP(2)**−**P*t*BA39** are plotted as blue triangles and red squares, respectively. The results of the convergent synthesis of **MOP(P*t*BA54)**, **MOP(P*t*BA148)**, and **MOP(P*t*BA272)** are plotted as black circles, black squares, and black tilted squares, respectively. The dashed line denotes the linear fitting of the results for **MOP(2)**−**P*t*BA39**.

of **MOP(2)**−**PSt22** were multimodal with a higher-molecular-weight shoulder (Figure 2c). However, as evidenced by the kinetic plots (Figure S7), the polystyrene arm chains underwent a controlled elongation, leading to a narrower polydispersity ($Đ \approx 1.2$). These contradictory observations could be due to star−star coupling[4c] because the termination reactions of styrene polymerization are dominated by combination reactions between living chain ends.[16] As a large number of living chains (theoretically 24 per core) are grafted from the single core, star−star coupling is very likely and sensitive to the probability of radical combination reactions. Thus, even a tiny rate of interstar radical combination may result in a considerable amount of star−star aggregates, leading to a multimodal peak with extremely high molecular weights.

Unlike **MOP(2)**, the solubility of **MOP(1)** was too low in any solvent to give a sufficient concentration for the polymerization reaction. However, **MOP(1)** was slightly dissolved in 1,4-dioxane in the presence of St monomers (1.6 mg/mL) (see Supporting Information), which allowed us to examine the RAFT polymerization of St mediated with **MOP(1)**. Although **MOP(1)** similarly provided **MOP(1)**−**PSt**, a considerably larger amount of free polymer was cogenerated (Figure S8). This free polymer formation is presumably caused by the low activation efficiency of the CT group in **MOP(1)** due to the poor solubility.

Convergent Route. Convergent synthesis is considered to be a facile and conventional way for preparation of dendrimers,[17] polymeric nanoparticles,[18] and star polymers[5−7] because it has the potential to reduce synthetic efforts. We examined a convergent synthesis (arm-first) approach (Figure 3a) using isophthalic acid-terminated poly(*t*BA) with a DP of 54, termed macroligand **P*t*BA54** ($M_{n,AC}$ (SEC) = 6700, $Đ$ = 1.11). **P*t*BA54** was prepared via conventional RAFT polymerization mediated with **2** (see Supporting Information). Interestingly, upon mixing **P*t*BA54** with copper(II) acetate in NMP, another macromolecular compound that had a higher molecular weight and quite narrow polydispersity was immediately formed (Figure 3b). This macromolecular product was attributed to the corresponding MOP-core CSP, termed **MOP(P*t*BA54)** ($M_{n,MOP}$ (SEC) = 62900, $Đ$ = 1.03).

To probe the limit of the macroligand length, we synthesized long precursor chains with an isophthalic acid end group, **P*t*BA148** ($M_{n,AC}$ (SEC) = 12700, $Đ$ = 1.25, DP = 148) and **P*t*BA272** ($M_{n,AC}$ (SEC) = 21800, $Đ$ = 1.27, DP = 272). In contrast to our assumption that longer macroligands are incapable of MOP-core formation because of steric congestion, even the longest **P*t*BA272** provided the corresponding MOP-core star polymer, termed **MOP(P*t*BA272)**, with an extremely high molecular weight and narrow polydispersity ($M_{n,MOP}$ (SEC) = 226300, $Đ$ = 1.10) (Figure S9). SEC-MALS analysis allowed us to determine the absolute $M_{w,MOP}$ (SEC-MALS) for **MOP(P*t*BA148)** and **MOP(P*t*BA272)** to be 522000 and 836000, which showed good agreement with the calculated values (Table 1). Unfortunately, the limit of the macroligand length has not yet been determined because the size-exclusion limit of SEC columns hampered the characterization of MOP formation from longer macroligands. The results for the convergent synthesis of MOP-core CSPs are summarized in Table 1.

The relationship between the $M_{n,MOP}$ and $M_{n,AC}$ values determined by SEC are plotted in Figure 3d. The dashed line denotes a linear fitting based on the RAFT polymerization results for **MOP(2)**−**P*t*BA39** (red squares), which shows that $M_{n,MOP}$ (SEC) is strictly proportional to $M_{n,AC}$ (SEC). This trend in the SEC data enabled us to prove the structural integrity of the star polymers synthesized via the convergent approach. The data for **MOP(P*t*BA54)**, **MOP(P*t*BA148)**, and **MOP(P*t*BA272)** are plotted in Figure 3d. These data are perfectly matched with the fit line, indicating that the MOP-core CSPs synthesized via the convergent approach have a star architecture that is identical to that obtained via the divergent approach. In fact, the **P*t*BA39** arm chain obtained by degrading **MOP(2)**−

DOI: 10.1021/jacs.6b01758
J. Am. Chem. Soc. 2016, 138, 6525−6531

P*t*BA39, which was originally synthesized via the divergent route, was used to successfully synthesis a CSP, namely **MOP(P*t*BA39)**, via the convergent route. The SEC profile of **MOP(P*t*BA39)** is superimposable on that of **MOP(2)−P*t*BA39** (Figure S10), which strongly indicates the equivalence of the divergent and convergent routes (see Supporting Information).

Mixed-Ligand Experiments. Using a mixed-ligand strategy, we were able to obtain miktoarm star polymers in one step. When a binary mixture of *n*-butyl acrylate, **P*n*BA56** (DP = 56), and **P*t*BA272** with a mixing molar ratio of 0.6:0.4 was reacted with copper(II) acetate (1.5 equiv to total amount of macroligands), the macroligands immediately converged into a single miktoarm CSP, termed **MOP(P*n*BA56$_{0.6}$/P*t*BA272$_{0.4}$)** (Figure 3a,c). The $M_{n,MOP}$ value of **MOP(P*n*BA56$_{0.6}$/P*t*BA272$_{0.4}$)** determined by SEC was between those of the homo star polymers of the respective macroligands, **MOP(P*n*BA56)** and **MOP(P*t*BA272)** (Table 1 and Figure S11), suggesting the statistical incorporation of the two different arms. **MOP(P*n*BA56$_{0.6}$/P*t*BA272$_{0.4}$)** was isolated from any unreacted free polymer by repeated precipitation in methanol/water (8:2, v/v) (Figure S12). To determine the incorporation ratio of the two arm chains, the isolated product was dissolved in deuterated acetone-d_6; the addition of a drop of DCl caused the star polymer to dissociate into the free arm chains. The actual incorporation ratios of **P*n*BA56** and **P*t*BA272** were determined using ^{1}H NMR measurements to be 0.62 and 0.38, respectively (Figure S13). The incorporation ratio was quite similar to the loading ratio, indicating that the coordination-driven self-assembly of these different length macroligands occurred equally in this regime. However, owing to the statistical nature of the convergent reaction, we should note that **MOP(P*n*BA56$_{0.6}$/P*t*BA272$_{0.4}$)** is not a discrete product and should have a distribution of constituents.

It should be noted that a small shoulder is occasionally observed by SEC in the higher-molecular-weight region for both the convergent and divergent CSPs (e.g., 13.5 min for **MOP(2)−P*t*BA39**, 13 min for **MOP(P*t*BA54)**, and 12 min for **MOP(P*n*BA56$_{0.6}$/P*t*BA272$_{0.4}$)**) (Figures 2b and 3b,c, respectively). The origin of this shoulder is at present unknown. One explanation for this peak could be the formation of star−star coupling aggregates, which are caused by trace contamination with telechelic byproducts formed via unfavorable radical polymerization side reactions.

In conventional star polymer syntheses, using either the divergent or convergent route, one has to modify the synthetic scheme to control the number of arm chains. In contrast, on MOP-core CSPs, the number of arm chains is easily tuned using the mixed-ligand method. Mixtures of macroligand **P*t*BA54** and coligand ***t*Bipa** at variable mixing ratios (**P*t*BA54**/***t*Bipa** = 3:21, 4:20, 6:18, 12:12, and 18:6) were reacted with copper(II) acetate in NMP, which readily gave corresponding MOP-core CSPs **MOP(P*t*BA54$_n$/*t*Bipa$_m$)** (***n*** and ***m*** denote the molar loading ratios of **P*t*BA54** and ***t*Bipa**, respectively; $n + m = 1$). After 60 min, the reaction mixture of each NMP solution was subjected to THF-SEC measurement. Figure 4a depicts the SEC results for **MOP(P*t*BA54$_n$/*t*Bipa$_m$)** (n = 1, 0.75, 0.5, 0.25, 0.167, 0.125, and 0, where n = 1 and 0 correspond to **MOP(P*t*BA54)** and **MOP(*t*Bipa)**, respectively).

As shown in the SEC traces, the peaks of the MOP-core CSPs shifted to lower molecular weights as the loading ratio of ***t*Bipa** increased. This observation clearly indicates that the ***t*Bipa** coligand was concomitantly incorporated onto the MOP core to

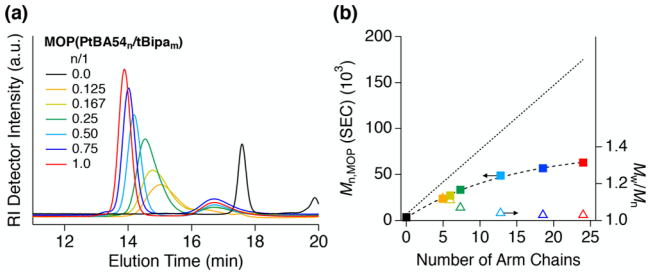

Figure 4. (a) THF-SEC traces for the reaction mixture of **MOP(P*t*BA54$_n$/*t*Bipa$_m$)**; n = 1, 0.75, 0.5, 0.25, 0.167, 0.125, and 0, where n = 1 and 0 correspond to **MOP(P*t*BA54)** and **MOP(*t*Bipa)**, respectively. (b) Relationship between $M_{n,MOP}$ determined by SEC for **MOP(P*t*BA54$_n$/*t*Bipa$_m$)** and the actual number of arm chains determined by ^{1}H NMR (square markers) (Figure S14). The colors of the markers correspond to the spectra in panel a. The dashed line denotes an exponential fit as a guide for the eyes. The theoretical relationship between $M_{n,MOP}$ (calcd) for **MOP(P*t*BA54$_n$/*t*Bipa$_m$)** and the number of arm chains is plotted as a dotted line.

"dilute" the arm chain density. Each star polymer was isolated from any free polymer by repeated precipitation in methanol/water (8:2, v/v). ^{1}H NMR measurements of each star polymer were performed in acetone-d_6 with a small aliquot of DCl to determine the incorporation number of **P*t*BA54** on the core, namely, the number of arm chains (Figure S14). The actual numbers of arm chains were determined to be 18.5, 12.8, 7.3, 6.0, and 4.9 for the respective **MOP(P*t*BA54$_n$/*t*Bipa$_m$)** (n = 0.75, 0.5, 0.25, 0.167, and 0.125). The actual numbers of arm chains were quite consistent with the loading ratios, indicating that the macroligand and small coligand have an equal chance of incorporation onto a single MOP core. Thus, this self-assembly process is independent of the ligand size in this composition range.

The relationship between $M_{n,MOP}$ determined by SEC of **MOP(P*t*BA54$_n$/*t*Bipa$_m$)** and the actual number of arm chains is plotted in Figure 4b. An exponential-like trend was observed, whereas a linear relationship with the number of arm chains is expected. The exponential-like trend is in contrast to the linear trend observed between $M_{n,MOP}$ and $M_{n,AC}$ (Figure 3d). Moreover, the polydispersity ($Đ = M_w/M_n$) determined by SEC becomes narrower as the number of arm chains increases (Figure 4b). These observations can be explained by the compact shape of the star polymers, as well as the known deviation from the linear calibration standards for the analysis of star polymers.[19] Moreover, the statistical convolution of the polymer polydispersities may play an additional role. Previous experimental and theoretical studies have demonstrated that the quantitative ligation of multiple polymers with similar polydispersities may result in a product that has a much lower polydispersity than those of the original polymers.[5b,20]

AFM Micrographs of Individual MOP-Core CSPs. Atomic force microscopy (AFM) was used to visualize the shape of individual CSPs (Figure 5a,b). We prepared a thin-film sample of **MOP(P*t*BA272)** by spin-casting a highly diluted chloroform solution (0.01 μg/mL) on a mica substrate. The individual molecules adopted a core−shell structure with so-called "sunny-side up egg" configuration (Figure 5c). Every particle was clearly shown to have an individual core that is covered by a polymeric corona (Figure 5b). The height of the inner core was ~2.5 nm, which is consistent with the diameter of **MOP(2)** (Figure 5d). This fact indicates that the cage-like structure of the MOP core is maintained in the dry state, even

DOI: 10.1021/jacs.6b01758
J. Am. Chem. Soc. 2016, 138, 6525−6531

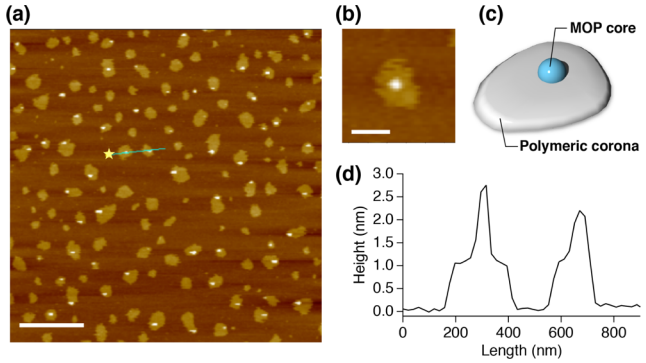

Figure 5. (a) AFM height image of individual particles of **MOP(PtBA272)** (scale bar = 1 μm). (b) Magnified view of a single particle of **MOP(PtBA272)** (scale bar = 100 nm). (c) Schematic diagram of so-called "sunny-side up egg" morphology. (d) Height profile along the green line in panel a, where the yellow star denotes the zero-length point.

after polymerization, thus retaining the internal cavity. It should be emphasized that this sophisticated macromolecular architecture is formed instantly in one step: mixing of isophthalic acid-terminated polymers and copper(II) ions in NMP at 25 °C.

At present, we have no rational way to determine the actual molecular weight distributions of CSPs, as discussed earlier. AFM micrographs could provide us with a visual insight regarding this issue. The individual CSP particles of **MOP(PtBA272)** have a wider size distribution than that deduced from the narrow polydispersity in the SEC analysis.

Bulk Structure of MOP-Core CSPs. Small-angle X-ray scattering (SAXS) measurements were employed to gain insight into the microstructure of the MOP-core CSPs in the bulk state. The SAXS profiles of **MOP(2)−PtBA15** and **MOP(2)−PtBA39** showed respective peaks at q = 0.145 and 0.103 Å^{-1}, which correspond to d-spacings of 4.33 and 6.13 nm, respectively (Figure 6a). The measurements were carried out at 25 °C, at which temperature, the CSPs are in the glassy state according to the glass transition temperature (T_g) of 41.8 °C determined by differential scanning calorimetry (DSC). A representative DSC curve for **MOP(2)−PtBA39** is shown in Figure S15. The observed d-spacings depended on the length of the polymer arms, indicating that each MOP core is spatially separated by the grafted polymeric arms (Figure 6c). The d-spacings, which can be interpreted as the diameter of the CSPs in the bulk state, are quite small compared with the diameters determined by DLS. This result suggests a densely packed organization of the CSPs with interdigitation of the arm chains in the bulk, although the single peak observed in the SAXS pattern is insufficient to determine the packing structures unambiguously.

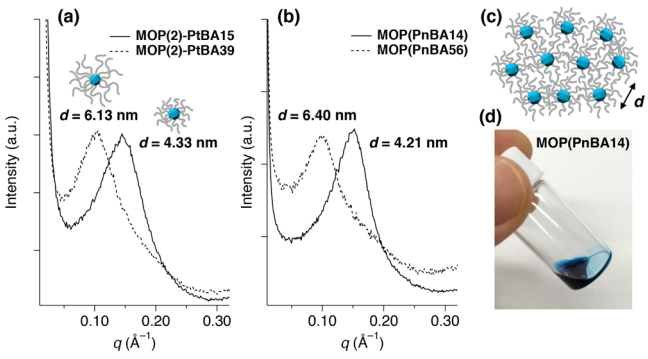

Figure 6. (a) SAXS profiles of bulk **MOP(2)−PtBA15** (solid line) and **MOP(2)−PtBA39** (dashed line) measured at 25 °C. (b) SAXS profiles of bulk **MOP(PnBA14)** (solid line) and **MOP(PnBA56)** (dashed line) measured at 25 °C. (c) Schematic diagram of the envisioned packing structure of MOP-core CSPs in the bulk state. The hexagonal-like arrangement of molecules adopted in the illustration is not supported by the SAXS data. (d) Visual appearance of **MOP(PnBA14)** at room temperature.

Interestingly, the MOP-core CSPs with n-butyl acrylate arms, **MOP(PnBA14)** and **MOP(PnBA56)**, also showed similar peaks in the SAXS profile, although these CSPs are viscous liquids at the measurement temperature (25 °C) (Figure 6b,d). The DSC curve of **MOP(PnBA14)**, which has a T_g of −43.7 °C, is depicted in Figure S15. **MOP(PnBA14)** and **MOP(PnBA56)** synthesized through the convergent method showed single peaks at q = 0.149 and 0.098 Å^{-1}, respectively, with d-spacings of 4.21 and 6.40 nm (Figure 6b). This polymer grafting technique realized an organized arrangement of coordination nanocages with a uniform inter-MOP distance, even in the liquid phase at ambient temperature. This approach could offer a new design principle for highly processable porous soft materials. Film fabrication and gas sorption tests on the MOP-core CSPs are now under way to validate their potential as a gas separation material.

CONCLUSION

In conclusion, we have shown both divergent and convergent synthesis of a new class of CSPs with metal−organic polyhedral cores. While the divergent route is accomplished through surface-initiated RAFT polymerization mediated with preformed multifunctional MOP cores, the convergent route readily provides the MOP-core star polymer via coordination-driven self-assembly of end-functionalized polymeric precursors (macroligand) and copper(II) ions. The latter method further enabled us to control the number of arm chains *in situ* and access a wide variety of star polymers, including miktoarm stars, with desired compositions in one step. Such MOP-core macromolecules may not only accelerate fundamental studies on polymer topologies but also open up a new field of CSPs. In addition, the MOP core, in which small molecules can be accommodated, provides many possible applications, including catalysis,[21] drug delivery,[11] molecular channels,[22] and gas separation.[12] The physical properties of MOP-core CSPs could be tuned by careful selection and precise control of the polymeric arms, which provides us with a design strategy for highly processable porous soft materials by using the coordination nanocages as a building component.

ASSOCIATED CONTENT

Supporting Information

The Supporting Information is available free of charge on the ACS Publications website at DOI: 10.1021/jacs.6b01758.

Synthesis and characterization, kinetic plots of RAFT polymerization, SEC traces, DLS data, electronic absorption spectra, ^{1}H NMR spectra, DSC curves, and FT-IR spectra (PDF)

AUTHOR INFORMATION

Corresponding Authors

*nhosono@icems.kyoto-u.ac.jp
*kitagawa@icems.kyoto-u.ac.jp

DOI: 10.1021/jacs.6b01758
J. Am. Chem. Soc. 2016, 138, 6525−6531

Present Addresses

[#]R.M.: Department of Applied Chemistry, Graduate School of Engineering, Nagoya University, Furo-cho, Chikusa, Nagoya 464-8603, Japan.

[§]H.S.: Department of Chemistry and Biotechnology, School of Engineering, The University of Tokyo, 7-3-1, Hongo, Bunkyo-ku, Tokyo 113-8656, Japan.

Notes

The authors declare no competing financial interest.

■ ACKNOWLEDGMENTS

This work was supported by KAKENHI Grant-in-Aid for Specially Promoted Research (No. 25000007) from the Japan Society of the Promotion of Science (JSPS) and the Regional Innovation Strategy Support Program (Next-generation Energy System Creation Strategy for Kyoto) from the Ministry of Education, Culture, Sports, Science and Technology (MEXT), Japan. N.H. acknowledges JSPS for KAKENHI Grant-in-Aid for Young Scientists (B) (No. 16K17959). R.M. thanks PRESTO program of the Japan Science and Technology Agency (JST) for the financial support. This work was also supported in part by the ACCEL program of JST. The authors thank Dr. T. Terashima and Mr. Y. Hirai for useful discussions and SEC-MALS measurements.

■ REFERENCES

(1) (a) Flory, P. J. *Principles of Polymer Chemistry*; Cornell University Press: Ithaca, NY, 1953. (b) Matyjaszewski, K.; Tsarevsky, N. V. *J. Am. Chem. Soc.* **2014**, *136*, 6513−6533.

(2) (a) Szwarc, M.; Levy, M.; Milkovich, R. *J. Am. Chem. Soc.* **1956**, *78*, 2656−2657. (b) Webster, O. W. *Science* **1991**, *251*, 887−893.

(3) (a) Matyjaszewski, K. *Polym. Int.* **2003**, *52*, 1559−1565. (b) Xue, L.; Agarwal, U. S.; Zhang, M.; Staal, B. B. P.; Müller, A. H. E.; Bailly, C. M. E.; Lemstra, P. J. *Macromolecules* **2005**, *38*, 2093−2100. (c) Boschmann, D.; Vana, P. *Macromolecules* **2007**, *40*, 2683−2693.

(4) (a) Xia, J.; Zhang, Z.; Matyjaszewski, K. *Macromolecules* **1999**, *32*, 4482−4484. (b) Baek, K.-Y.; Kamigaito, M.; Sawamoto, M. *Macromolecules* **2001**, *34*, 215−221. (c) Chaffey-Millar, H.; Stenzel, M. H.; Davis, T. P.; Coote, M. L.; Barner-Kowollik, C. *Macromolecules* **2006**, *39*, 6406−419. (d) Terashima, T.; Nishioka, S.; Koda, Y.; Takenaka, M.; Sawamoto, M. *J. Am. Chem. Soc.* **2014**, *136*, 10254−10257.

(5) (a) Huang, F.; Nagvekar, D. S.; Slebodnick, C.; Gibson, H. W. *J. Am. Chem. Soc.* **2005**, *127*, 484−485. (b) Todd, E. M.; Zimmerman, S. C. *J. Am. Chem. Soc.* **2007**, *129*, 14534−14535. (c) Chen, S.; Bertrand, A.; Chang, X.; Alcouffe, P.; Ladavière, C.; Gérard, J.-M.; Lortie, F.; Bernard, J. *Macromolecules* **2010**, *43*, 5981−5988. (d) Schmidt, B. V. K. J.; Rudolph, T.; Hetzer, M.; Ritter, H.; Schacher, F. H.; Barner-Kowollik, C. *Polym. Chem.* **2012**, *3*, 3139−3145.

(6) (a) Wu, X.; Fraser, C. L. *Macromolecules* **2000**, *33*, 4053−4060. (b) Moughton, O. M.; O'Reilly, R. K. *Macromol. Rapid Commun.* **2010**, *31*, 37−52. (c) Li, D.; Li, H.; Wu, L. *Polym. Chem.* **2014**, *5*, 1930−1937.

(7) (a) Deng, G.; Ma, D.; Xu, Z. *Eur. Polym. J.* **2007**, *43*, 1179−1187. (b) Khanna, K.; Varshney, S.; Kakkar, S. *Polym. Chem.* **2010**, *1*, 1171−1185. (c) Schmidt, B. V. K. J.; Hetzer, M.; Ritter, H.; Barner-Kowollik, C. *Polym. Chem.* **2012**, *3*, 3064−3067.

(8) (a) Yaghi, O. M.; O'Keeffe, M.; Ockwig, N. W.; Chae, H. K.; Eddaoudi, M.; Kim, J. *Nature* **2003**, *423*, 705. (b) Kitagawa, S.; Kitaura, R.; Noro, S. *Angew. Chem., Int. Ed.* **2004**, *43*, 2334−2375. (c) Uemura, T.; Horike, S.; Kitagawa, S. *Chem. - Asian J.* **2006**, *1*, 36−44. (d) Horike, S.; Dincă, M.; Tamaki, K.; Long, J. R. *J. Am. Chem. Soc.* **2008**, *130*, 5854−5855. (e) Li, L.; Matsuda, R.; Tanaka, I.; Sato, H.; Kanoo, P.; Jeon, H. J.; Foo, M. W.; Wakamiya, A.; Murata, Y.; Kitagawa, S. *J. Am. Chem. Soc.* **2014**, *136*, 7543−7546. (f) Diring, S.; Wang, D. O.; Kim, C.; Kondo, M.; Chen, Y.; Kitagawa, S.; Kamei, K.-i.; Furukawa, S. *Nat. Commun.* **2013**, *4*, 2684. (g) Sato, H.; Kosaka, W.; Matsuda, R.; Hori, A.; Hijikata, Y.; Belosludov, R. V.; Sakaki, S.; Takata, M.; Kitagawa, S. *Science* **2014**, *343*, 167−170.

(9) (a) Eddaoudi, M.; Kim, J.; Wachter, J. B.; Chae, H. K.; O'Keeffe, M.; Yaghi, O. M. *J. Am. Chem. Soc.* **2001**, *123*, 4368−4369. (b) Furukawa, H.; Kim, J.; Plass, K. E.; Yaghi, O. M. *J. Am. Chem. Soc.* **2006**, *128*, 8398−8399. (c) Larsen, R. W. *J. Am. Chem. Soc.* **2008**, *130*, 11246−11247. (d) Tranchemontagne, D. J.; Ni, Z.; O'Keeffe, M.; Yaghi, O. M. *Angew. Chem., Int. Ed.* **2008**, *47*, 5136−5147. (e) Li, J. R.; Zhou, H.-C. *Nat. Chem.* **2010**, *2*, 893−898.

(10) (a) Perry, J. J., IV; Kravtsov, V. Ch.; McManus, G. J.; Zaworotko, M. J. *J. Am. Chem. Soc.* **2007**, *129*, 10076−10077. (b) Perry, J. J., IV; Perman, J. A.; Zaworotko, M. J. *Chem. Soc. Rev.* **2009**, *38*, 1400−1417.

(11) (a) Zhao, D.; Tan, S.; Yuan, D.; Lu, W.; Rezenom, Y. H.; Jiang, H.; Wang, L.-Q.; Zhou, H.-C. *Adv. Mater.* **2011**, *23*, 90−93. (b) Mallick, A.; Garai, B.; Díaz Díaz, D.; Banerjee, R. *Angew. Chem., Int. Ed.* **2013**, *52*, 13755−13759.

(12) (a) Perez, E. V.; Balkus, K. J.; Ferraris, J. P.; Musselman, I. H. *J. Membr. Sci.* **2014**, *463*, 82−93. (b) Zhao, C.; Wang, N.; Wang, L.; Huang, H.; Zhang, R.; Yang, F.; Xie, Y.; Ji, S.; Li, J.-R. *Chem. Commun.* **2014**, *50*, 13921−13923. (c) Ma, J.; Ying, Y.; Yang, Q.; Ban, Y.; Huang, H.; Guo, X.; Xiao, Y.; Liu, D.; Li, Y.; Yang, W.; Zhong, C. *Chem. Commun.* **2015**, *51*, 4249−4251.

(13) (a) Olenyuk, B.; Whiteford, J. A.; Fechtenkötter, A.; Stang, P. J. *Nature* **1999**, *398*, 796−799. (b) Northrop, B. H.; Zheng, Y.-R.; Chi, K.-W.; Stang, P. J. *Acc. Chem. Res.* **2009**, *42*, 1554−1563. (c) Tominaga, M.; Suzuki, K.; Kawano, M.; Kusukawa, T.; Ozeki, T.; Sakamoto, S.; Yamaguchi, K.; Fujita, M. *Angew. Chem., Int. Ed.* **2004**, *43*, 5621−5625. (d) Kamiya, N.; Tominaga, M.; Sato, S.; Fujita, M. *J. Am. Chem. Soc.* **2007**, *129*, 3816−3817.

(14) (a) Chong, B. Y. K.; Krstina, J.; Le, T. P. T.; Moad, G.; Postma, A.; Rizzardo, E.; Thang, S. H. *Macromolecules* **2003**, *36*, 2256−2272. (b) Moad, G.; Chong, Y. K.; Postma, A.; Rizzardo, E.; Thang, S. H. *Polymer* **2005**, *46*, 8458−8468. (c) Li, C.; Han, J.; Ryu, C. Y.; Benicewicz, B. C. *Macromolecules* **2006**, *39*, 3175−3183.

(15) (a) Junkers, T.; Barner-Kowollik, C. *J. Polym. Sci., Part A: Polym. Chem.* **2008**, *46*, 7585. (b) Koo, S. P. S.; Junkers, T.; Barner-Kowollik, C. *Macromolecules* **2009**, *42*, 62−69.

(16) (a) Zammit, M. D.; Davis, T. P.; Haddleton, D. M.; Suddaby, K. G. *Macromolecules* **1997**, *30*, 1915−1920. (b) Nakamura, Y.; Yamago, S. *Macromolecules* **2015**, *48*, 6450−6456.

(17) (a) Grayson, S. M.; Fréchet, J. M. J. *Chem. Rev.* **2001**, *101*, 3819−3868. (b) Hawker, C. J.; Fréchet, J. M. J. *J. Am. Chem. Soc.* **1990**, *112*, 7638−7647. (c) Xu, L.; Chen, L. J.; Yang, H.-B. *Chem. Commun.* **2014**, *50*, 5156−5170.

(18) (a) Hermans, T. M.; Broeren, M. A. C.; Gomopoulos, N.; van der Schoot, P.; van Genderen, M. H. P.; Sommerdijk, N. A. J. M.; Fytas, G.; Meijer, E. W. *Nat. Nanotechnol.* **2009**, *4*, 721−726. (b) Liao, L.; Liu, J.; Dreaden, E. C.; Morton, S. W.; Shopsowitz, K. E.; Hammond, P. T.; Johnson, J. A. *J. Am. Chem. Soc.* **2014**, *136*, 5896−5899.

(19) (a) Stenzel, M. H.; Davis, T. P. *J. Polym. Sci., Part A: Polym. Chem.* **2002**, *40*, 4498. (b) Hawker, C. J.; Fréchet, J. M. J. *J. Am. Chem. Soc.* **1990**, *112*, 7638.

(20) (a) Barner-Kowollik, C. *Macromol. Rapid Commun.* **2009**, *30*, 1625−1631.

(21) (a) Murase, T.; Nishijima, Y.; Fujita, M. *J. Am. Chem. Soc.* **2012**, *134*, 162−164. (b) Vardhan, H.; Verpoort, F. *Adv. Synth. Catal.* **2015**, *357*, 1351−1368.

(22) Jung, M.; Kim, H.; Baek, K.; Kim, K. *Angew. Chem., Int. Ed.* **2008**, *47*, 5755−5757.

DOI: 10.1021/jacs.6b01758
J. Am. Chem. Soc. 2016, 138, 6525−6531